

## 1 **Size matters: large copy number losses reveal novel Hirschsprung disease genes**

2 Laura Kuil<sup>1</sup>, Katherine C. MacKenzie<sup>1</sup>, Clara S Tang<sup>3,4</sup>, Jonathan D. Windster<sup>1,2</sup>, Thuy Linh Le<sup>5</sup>, Anwarul  
3 Karim<sup>3</sup> Bianca M. de Graaf<sup>1</sup>, Robert van der Helm<sup>1</sup>, Yolande van Bever<sup>1</sup>, Cornelius E.J. Sloots<sup>2</sup>, Conny  
4 Meeussen<sup>2</sup>, Dick Tibboel<sup>2</sup>, Annelies de Klein<sup>1</sup>, René M. H. Wijnen<sup>2</sup>, Jeanne Amiel<sup>5</sup>, Stanislas Lyonnet<sup>5</sup>,  
5 <sup>7</sup>, Maria-Mercè Garcia-Barcelo<sup>3</sup>, Paul K.H. Tam<sup>3,4</sup>, Maria M. Alves<sup>1</sup>, Alice Brooks<sup>1</sup>, Robert M.W. Hofstra<sup>1</sup>,  
6 <sup>6</sup>, Erwin Brosens<sup>1\*</sup>

7 <sup>1</sup>Department of Clinical Genetics, Erasmus University Medical Centre Rotterdam, The Netherlands.

8 <sup>2</sup>Department of Paediatric Surgery, Erasmus University Medical Centre, Rotterdam, The Netherlands.

9 <sup>3</sup>Department of Surgery, Li Ka Shing Faculty of Medicine, The University of Hong Kong, Hong Kong, China.

10 <sup>4</sup>Li Dak-Sum Research Centre, The University of Hong Kong – Karolinska Institutet Collaboration in Regenerative Medicine, Hong  
11 Kong, China

12 <sup>5</sup>Laboratory of embryology and genetics of malformations, Institut Imagine, Université de Paris, INSERM UMR1163, Necker  
13 Enfants malades University Hospital, APHP, Paris, France.

14 <sup>6</sup>Stem Cells and Regenerative Medicine, UCL Great Ormond Street Institute of Child Health, London, UK

15 \* corresponding author: [e.brosens@erasmusmc.nl](mailto:e.brosens@erasmusmc.nl)

16

### 17 **Abstract**

#### 18 *Background*

19 Hirschsprung disease (HSCR) is characterized by absence of ganglia in the intestine. Approximately  
20 18% of patients have additional anatomical malformations or neurological symptoms (HSCR-AAM).  
21 HSCR is a complex genetic disease in which the loss of enteric ganglia stems from a combination of  
22 genetic alterations: rare coding variants, predisposing haplotypes and Copy Number Variation (CNV).  
23 Pinpointing the responsible culprits within a large CNV is challenging as often many genes are  
24 affected. We investigated if we could find deleterious CNVs and if we could identify the genes  
25 responsible for the aganglionosis.

#### 26 *Results*

27 Deleterious CNVs were detected in three groups of patients: HSCR-AAM, HSCR patients with a  
28 confirmed causal genetic variant and HSCR-isolated patients without a known causal variant and  
29 controls. Predisposing haplotypes were determined, confirming that every HSCR subgroup had  
30 increased contributions of predisposing haplotypes, but their contribution was highest in isolated  
31 HSCR patients without *RET* coding variants. CNV profiling proved that HSCR-AAM patients had larger  
32 copy number losses. Gene enrichment strategies using mouse enteric nervous system transcriptomes  
33 and constraint metrics were used to determine plausible candidate genes in Copy Number Losses.  
34 Validation in zebrafish using CRISPR/Cas9 targeting confirmed the contribution of *UFD1L*, *TBX2*,

**NOTE: This preprint reports new research that has not been certified by peer review and should not be used to guide clinical practice.**

35 *SLC8A1* and *MAPK8* to ENS development. In addition, we revealed epistasis between reduced Ret  
36 and Gnl1 expression *in vivo*.

37 *Conclusion*

38 Rare large Copy Number losses - often *de novo* - contribute to the disease in HSCR-AAM patients  
39 specifically. We proved the involvement of five genes in enteric nervous system development and  
40 Hirschsprung disease.

## 41 Introduction

42 Hirschsprung disease (HSCR) is characterized by absence of the enteric nervous system (ENS) in the  
43 intestine (aganglionosis). HSCR is a complex genetic disease where the phenotype stems from a  
44 combination of genetic alterations: rare coding variants, predisposing haplotypes and Copy Number  
45 Variation (CNV)[1]. Most patients have HSCR as an isolated congenital anomaly, while in others the  
46 absence of enteric neurons is part of a spectrum of anomalies of a monogenetic syndrome[2].  
47 Approximately 18% of patients have additional anatomical malformations or neurological symptoms[3]  
48 (HSCR-AAM). Deletions of 10q11[4, 5] led to the identification of the REarranged during Transfection  
49 gene (*RET*), the major responsible gene for familial and sporadic isolated HSCR[6, 7]. HSCR  
50 penetrance is influenced by predisposing *RET* risk haplotypes which increase disease risk  
51 substantially, especially if homozygous, in specific combinations (rs2506030, rs7069590,  
52 rs2435357)[8, 9], together with other risk loci near the semaphorin gene cluster (rs80227144)[9, 10],  
53 or the neuregulin 1 gene (*NRG1*; rs7005606)[11-13].

54 For many of HSCR-AAM patients the underlying cause is unknown. It is plausible that the associated  
55 anomalies in these patients are the result of a pathogenic single nucleotide variant or  
56 insertion/deletion. However, all different genomic variation types should be considered, since the  
57 presence of unbalanced translocations and CNV has resulted in the identification of causal genes for  
58 several syndromes with HSCR as a key feature. For example, deletions of 13q[1, 14-18] resulted in  
59 the identification of one of the genes responsible for Waardenburg-Shah syndrome type 4  
60 (*EDNRB*)[19]. Deletions of 2q[20-23] and 4p[24] contributed to the discovery of genes responsible for  
61 Mowatt-Wilson syndrome (*ZEB2*, formerly *ZFHX1B*)[25] and the gene responsible for Congenital  
62 Central Hypoventilation Syndrome (*PHOX2B*)[26]. Furthermore, deletions (17q21[27] and 22q11[1,  
63 28]) and duplications (17q23[29], dup22p[27, 30] and 22q11[31]) have been described in HSCR  
64 patients. In the light of these findings, we hypothesized that rare CNVs significantly contribute to  
65 aganglionosis in HSCR-AAM patients who lack a pathogenic coding variant in any of the known HSCR  
66 genes.

67

## 68 Results

### 69 *Rare deletions are enriched in HSCR-AAM patients*

70 Patient and control CNVs were determined and classified as a “rare CNV” when absent from  
71 large control cohorts (n=19,584). We also included known pathogenic or modifier CNVs[32, 33]. The  
72 size, type and gene content characteristics of rare CNVs were compared to those of 326 controls  
73 (Group 4, n=326). With this approach, 56 rare CNVs were detected in 34 HSCR patients (S3). We  
74 determined segregation of the rare CNVs in nine patients, five of these were *de novo*: three gains  
75 (22q11.21 - q11.22, 22q11.21 and 7q36.1) and two losses (17q23.1 - q23.2 and 6p22.1 - p21.33).  
76 CNV regions did not have a lot of overlap within our cohort, previously published CNV studies or with  
77 those described in the DECIPHER (<https://decipher.sanger.ac.uk/>) database (S3). The number of rare  
78 CNVs per individual did not differ between subgroups or controls (S4). However, CNVs found in  
79 HSCR-AAM patients (Group 1) were larger compared to controls (Group 4,  $p=7.297E-6$ , Figure 2A).  
80 This difference is attributed to outliers, large size of losses in specific patients of group 1 ( $p=3.15E-$   
81  $08$ )(S5), strongly suggesting a role of these specific CNVs in HSCR-AAM patients.

### 82 *Candidate genes within a loss are constraint and expressed during ENS development*

83 HSCR disease genes (S6) are often constraint and expressed in the affected tissue, genes  
84 within a CNV region associated with HSCR should share these characteristics (Figure 1A). In Group 1,  
85 rare CNVs are enriched for ENS genes ( $p=4.565E-6$ , S7). Moreover, losses in HSCR-AAM patients  
86 (Group 1) contained more ENS genes that are constraint[34, 35], compared to losses found in  
87 controls (Group 4, Figure 2B,  $p=0,0004$ ). Therefore, constraint genes within CN losses identified in  
88 group 1, and expressed in the ENS were prioritized as candidate genes for HSCR: *AKT3*, *GNL1*,  
89 *GABBR1*, *SLC8A1*, *MAPK8*, *UFD1L*, *TBX2*, *USP32* and *TUBB* (Table 1).

### 90 *Zebrafish validation confirms the impact of candidate gene disruption on ENS development*

91 To validate the effect of losing one copy of these constraint genes in ENS development and  
92 HSCR, we disrupted their orthologues in zebrafish by CRISPR/Cas9 targeting. Zebrafish are highly  
93 suited for reverse-genetic screening due to their rapid, *ex-utero* development and transparency and  
94 have proven instrumental in the identification of HSCR disease genes[36]. Premature termination of  
95 enteric neuron migration was observed in a subgroup of larvae injected with guide RNAs targeting  
96 *ufd1l* ( $p=0,0208$ ), *tbx2* ( $p=0,0373$ ), *slc8a1* ( $p=0,0073$ ), and *mapk8* ( $p=0,0022$ , Figure 2D).

97 *HSCR disease coding genetics is heterogeneous*

98 More evidence for their involvement could be provided by finding additional patients with  
99 putative deleterious alterations in genes affected by rare CNV. However, there was no significant  
100 enrichment for nonsense, splice site or missense variants in genes impacted by rare gains nor losses  
101 (S9) when comparing 443 short segment HSCR patients and 493 controls[37], underlining the genetic  
102 heterogeneity between HSCR patients. Nonsense or splice-site variants were detected in eight genes  
103 (Table 2). Only one variant, detected in DNA derived from blood and isolated ENS cells, affected a  
104 constraint gene overexpressed in the mouse ENS and present in a CN loss: a frameshift (*TUBB*;  
105 NM\_001293212.1:c.1330\_1331delCAinsA, p.Gln444Serfs\*35) in a patient with isolated HSCR (table  
106 1, S8).

107 *Copy number loss alone is likely not sufficient to result in HSCR*

108 Considering that aganglionosis has a low prevalence in patients with 22q11[32, 33, 38] and  
109 17q23[39, 40] deletions, CNVs alone are probably not sufficient to cause HSCR. HSCR penetrance is  
110 influenced by predisposing risk haplotypes [8-13]. Five non-coding risk haplotypes were tested in our  
111 three patient groups and compared to an *in-house* population dataset (group 5) (n=727, Risk non-  
112 coding (RSnc) =2.54). As expected, HSCR groups 1, 2 and 3 all had a higher RSnc compared to  
113 group 5 ( $p=4.59825E-14$ ,  $p=0.000960603$ ,  $p=1.21875E-23$ , respectively) (Figure 2C), indicating a  
114 contribution of the risk haplotypes in all HSCR subgroups. (S10; Figure 1B). Associated common risk  
115 haplotypes have epistatic interactions, not only with each other, but also with known HSCR genes -  
116 such as *RET* and *NRG1*[10, 12, 41] - and modify HSCR penetrance in monogenetic syndromes and  
117 Down syndrome[42-46]. The effect of epistatic interactions is smaller in high penetrant HSCR  
118 monogenetic disorders and larger in disorders in which HSCR penetrance is lower[42, 43]. In line with  
119 this, contribution of these risk haplotypes was the lowest in group 2 (RSnc=3.70), followed by group 1  
120 (RSnc=4.71), and the highest in group 3 (RSnc= 5.66). Thus, risk haplotypes have indeed a higher  
121 impact in HSCR patients without known coding variants, compared to those that contain known coding  
122 variants (S11). To model reduced *RET* expression in patients with predisposing haplotypes, we  
123 injected zebrafish with an antisense ATG blocking morpholino specific for *ret*. Disruption of the  
124 candidate genes *mapk8* ( $p=0,011$ , Figure 2E) and *gnl1* ( $p=0,0405$ , Figure 2F) in combination with the  
125 *ret* morpholino resulted in less neurons. Considering that disruption of *gnl1* alone did not induce a

126 HSCR phenotype, these results suggest that only in a sensitized background loss of *gnl1* can increase  
127 HSCR penetrance.

128 *Candidate genes are associated to ENS development.*

129 CRISPR/CAS9 targeted knockdown of the candidate genes *SLC8A1*, *GNL1*, *MAPK8*, *UFD1L*  
130 and *TBX2* connects these genes to ENS development. These genes are overexpressed in mouse  
131 ENS and have associations to ENS development. For instance, Mitogen-Activated Protein Kinase 8  
132 gene (*MAPK8*) is part of the Mitogen activated protein (MAP) kinase pathway and required for ENCCs  
133 to migrate properly[47]. *UFD1L*, as this encodes for a downstream target of *HAND2*[48]. *Hand2*<sup>-/-</sup> mice  
134 have decreased numbers of enteric neurons, neuronal differentiation defects and a disorganized  
135 ENS[49, 50]. T-Box 2 (*TBX2*) codes for a transcription factor already known to be involved in the  
136 regulation of neural crest derived melanocytes[51], a process that is also hampered in specific HSCR  
137 patients carrying pathogenic variants in *EDN3*, *SOX10* and *EDNRB*[52, 53]. Candidate genes are  
138 discussed further in S8.

## 139 **Discussion**

140 The results presented here highlight the importance of Copy Number profiling, leading us to  
141 propose a HSCR risk model that consists of risk scores for: rare coding variants, non-coding variants,  
142 rare CNVs and currently unknown risk factors (e.g. epigenetic modifications and perhaps  
143 environmental factors). Considering HSCR-AAM (group 1), 36% of patients have contained a CNV  
144 harboring genes overexpressed in the mouse ENS (Figure 3A). Our risk model (Figure 3C) indicates  
145 major contributing factors in each group: in group 1 CNVs, in group 2 coding variants and in group 3  
146 noncoding variants (Figure 3A, C). The predisposing *RET* haplotypes reduce *RET* expression[54] and  
147 in combination with the other risk haplotypes increase HSCR risk substantially. Translating this  
148 population risk to a threshold for HSCR development in individual patients is challenging as it is not  
149 precisely known how many of (and if) these known predisposing haplotypes are sufficient to result in  
150 aganglionosis. If we set a threshold at a relatively high level (RSnc>6), this would explain HSCR in  
151 30% of patients in group 3 (S11, Figure 2C, 3A). Most HSCR-AAM patients have a lower RSnc, which  
152 makes sense, as this group contains more high impact CNVs and whilst they lack *RET* coding  
153 variants, they potentially have variants in other genes (Figure 2C, 3A, S11). Translating our findings  
154 back to our full cohort including all patients seen by a clinical geneticist and screened for *RET*

155 mutations, HSCR coding variants explain 21% of HSCR cases (Figure 3B). If we consider CNVs  
156 containing genes expressed in the ENS, we could explain an additional 10% (Figure 3B). Importantly,  
157 this is an underestimation, since for 55% of patients without a *RET* coding variant no copy number  
158 profiling is performed (Figure 3B) and we focussed exclusively on rare CNVs. Since more common  
159 CNVs can also modify HSCR penetrance[55, 56], our results emphasize the need for a more  
160 widespread genomic analyses in all subgroups. Noncoding risk scores could be one of the  
161 determinants for a more elaborate genetic evaluation. A high noncoding risk score in a HSCR patient  
162 without associated anomalies is less likely to have a deleterious *RET* coding variant, patients with a  
163 low score are more likely to benefit from exome sequencing. Similarly, patients with large *de novo*  
164 losses often have a more complex phenotype and more intensive clinical investigations might be  
165 indicated.

## 166 **Conclusions**

167 To summarize, HSCR genetics is complex with contributions of predisposing haplotypes in all  
168 HSCR subgroups. Rare large CNVs - often *de novo* (S5) - contribute substantially to the disease in  
169 HSCR-AAM patients. These CNVs are enriched for CN losses and for genes intolerant to variation  
170 that are overexpressed in the developing mouse ENS. Disruption of some of these genes in zebrafish  
171 confirmed that reduced expression of these genes increased the occurrence of HSCR, alone, or in  
172 epistasis with *Ret*. These genes have functional overlap with known HSCR disease genes: e.g.  
173 *UFD1L* is involved signalling receptor binding and *MAPK8* in axon guidance. Our “ENS expressed  
174 gene” based approach lead to the identification of new HSCR disease genes (Figure 3; Table 2):  
175 *UFD1L*, *TBX2*, *SLC8A1*, *GNL1* and *MAPK8*.

## 176 **Materials and methods**

177 All authors had access to the study data and reviewed and approved the final manuscript

### 178 **Patient inclusion**

179 This project was approved by the Medical ethics committee of the Erasmus Medical Centre  
180 (Hirschsprung disease: no 2012-582, addendum No. 1 and no.193.948/2000/159, addendum No. 1  
181 and 2, MEC-20122387). We selected 58 out of 197 patients (Figure 3) for which DNA and informed  
182 consent were available, and in whom *RET* was screened. Three subgroups of HSCR patients were

183 included in the CNV detection study: patients with HSCR and additional anatomical malformations or  
184 neurological defects, but without a *RET* pathogenic variant, or other causal genetic defect (group 1,  
185 n=23, S1), patients with HSCR and a known variant in *RET* or another causal gene (group 2, n=15,  
186 S2), and patients with only HSCR, without a deleterious *RET* coding variant or other causal genetic  
187 defect (group 3, n=20). Additionally, we included unaffected control individuals (group 4, n=326).  
188 Genotypes of noncoding predisposing loci were compared with those of other unaffected controls  
189 (group 5, n=727).

#### 190 **Determination of Copy Number Variation (Figure 1a)**

191 CNV profiles were determined with either the HumanCytoSNP-12 v2.1 or the Infinium Global  
192 Screening Array-24 v1.0 (Illumina Inc., San Diego, CA, USA), using methods previously described[57].  
193 CNV profiles were inspected visually in Biodiscovery Nexus CN8.0 (Biodiscovery Inc., Hawthorne, CA,  
194 USA). CNVs with an overlap of at least 75% with similar state CN changes, were either classified as  
195 rare, when absent from large control cohorts (n=19,584), or as a known modifier[32, 33]. CNV  
196 number, size, type and gene content of rare CNVs were determined in HSCR patients (n=58) and  
197 unaffected controls (n=326) and compared between the control groups and previously described  
198 HSCR subgroups. All rare CNVs were uploaded to the ClinVar database  
199 (<https://www.ncbi.nlm.nih.gov/clinvar/>) and are depicted in S3.

#### 200 **Exclusion of the involvement of known disease genes (Figure 1a)**

201 The presence of *RET* coding mutations and those in intron-exon boundaries, in all patients in this  
202 study are determined. Furthermore, if a specific monogenetic syndrome (S6) was suspected based on  
203 the phenotypic spectrum observed, the suspected gene(s) were evaluated using a targeted NGS  
204 panel or whole exome sequencing. In four HSCR patients with associated anomalies (Group 1) and  
205 nine HSCR patients without associated anomalies (Group 3), the involvement of other known disease  
206 genes was excluded[2, 36, 37, 58] using whole exome sequencing (WES) with previously described  
207 pipelines[59, 60] and variant prioritization methods[61].

#### 208 **Evaluation of candidate gene expression (Figure 1a)**

209 We prioritized candidate genes based on gene characteristics: genes that are intolerant to variation  
210 and/or dosage sensitive (see variant filter criteria), and overexpressed in the developing mouse ENS  
211 compared to whole gut, between embryonic day E11.5 and E15.5 [62, 63]. Since data from human



212 colon was only available for embryonic week 12, 14 and 16, we evaluated gene expression in these  
213 time points[64]. Data was downloaded from the gene expression omnibus (GSE34208 and  
214 GSE100130). Genes that were dosage sensitive, and either overexpressed in the mouse ENS or  
215 highly expressed in human embryonic colon, were selected.

### 216 **Variant prioritization in loss of function genes (Figure 1a)**

217 To determine whether a gene affected by a rare putative deleterious CNV was constraint[34, 35], we  
218 allowed some tolerance to account for reduced penetrance (S9). Variants from NGS data previously  
219 generated were prioritized according to settings described in S9: These data included a WES cohort of  
220 sporadic HSCR (n=76, 149 controls) and (2) a Whole Genome Sequencing (WGS) cohort of 443 short  
221 segment HSCR patients and 493 unaffected controls[37]. Using RVTESTS[65], a variant burden test  
222 was done comparing the variant burden in 443 short segment HSCR patients and 493 controls (S9).  
223 All rare putative deleterious loss of function variants unique to the HSCR cohort in constraint genes  
224 are described in table 1.

### 225 **Genotyping of HSCR associated SNPs**

226 Sanger sequencing was used to genotype all patients for SNPs known to be associated to HSCR[8-  
227 10, 55]. Primer sequences can be found in S11. We used (proxy) SNPs present on the GSAMD-v1  
228 chip to determine the Rotterdam population background for these risk haplotypes (S10).

### 229 **Experimental animals**

230 Zebrafish were kept on a 14h/10h light–dark cycle at 28°C, during development and adulthood.  
231 Tg(*phox2bb*:GFP) animals were used for all experiments[66]. Larvae were kept in HEPES-buffered E3  
232 medium and 0.003% 1-phenyl 2-thiourea (PTU) was added 24 hours post fertilization (hpf), to prevent  
233 pigmentation.

### 234 **CRISPR/Cas9 gene disruption**

235 Gene targeting using CRISPR/Cas9 was performed as described previously[67]. The Alt-R CRISPR-  
236 Cas9 System from Integrated DNA Technologies (IDT) was used[68] (Figure 2A). crRNAs were  
237 designed using the IDT tool and selected on high target efficiency and low off target effect. gRNA  
238 sequences are listed in S13, primers used are listed in supplementary S14. Efficiency of indel  
239 generation was determined as described previously[67] (S15).

## 240 **Morpholino injections**

241 Fertilized zebrafish eggs were injected with the CRISPR/Cas9 complex. Subsequently, 0,5 or 1 ng of  
242 translation blocking morpholino against *ret* (5'- ACACGATTCCCCGCGTACTTCCCAT -3'), and 1:10  
243 Phenol Red (Sigma-Aldrich), was injected between the 1- and 4-cell stage (see figure 2D)[69]. To  
244 minimize variability, the same needle was used to inject the controls, that were not injected with  
245 CRISPR/Cas9 complex.

## 246 **Imaging**

247 Images of 5 dpf tg(*phox2bb*:GFP) larvae were taken using a Leica M165 fluorescent dissection  
248 microscope with the Leica LASX software. Larvae were anesthetized with 0.016% MS-222 in HEPES  
249 buffered E3 medium and positioned on their lateral side on a 1.5 - 2% agarose coated petridish, to  
250 enable visualization of the enteric neurons.

## 251 **Scoring HSCR phenotypes in zebrafish**

252 To determine whether the larvae present with a HSCR phenotype five categories were made: normal,  
253 hypoganglionic (less neurons), ultra-short segment HSCR (only most distal end of the gut lack  
254 neurons), short segment HSCR (neurons colonize until the midgut), and total colonic HSCR (neurons  
255 are absent from the total intestine) (see figure 2C).

## 256 **Statistical analysis**

257 The number and size of rare CNVs, the number of rare losses and gains, the number of genes  
258 intolerant to variation (SNVs and CNVs), the number of genes overexpressed in mouse ENS per rare  
259 CNV, and the relative weighted risk score, were determined and compared for the different groups  
260 with a single ANOVA test. If group differences existed ( $P < 0.05$ ), we determined which subgroups were  
261 significantly different, using a two-tailed T-test. For statistical analysis of the zebrafish experiments the  
262 online tool MedCalc (MedCalc software ltd., Ostend, Belgium), was used together with the "N-1" Chi-  
263 squared test, number of larvae used and p values can be found in supplementary S16.

## 264 **Supplemental Data description**

265 CNV\_HSCR\_MedRxiv\_Kuil\_etal\_supplement contains 16 elements including detailed patients  
266 descriptions, additional results, extended methods, primers and gRNA sequences.

## 267 **Author Contributions**

268 Guarantor of the article [EB]; Conception or design of the work [EB, AB, RH], the acquisition [RW, JW,  
269 TL, RH, YB, CS, CM, DT, LK], analysis [LK, KM, CT, BM, AK], or interpretation [EB, LK, CT] of data;  
270 drafted the work [EB, KM, LK] or substantively revised it [MA, RH, AB, JA, SL, MB, PT].

#### 271 **Acknowledgements**

272 This study makes use of data generated by the DECIPHER community[70]. A full list of centers who  
273 contributed to the generation of the data is available from <http://decipher.sanger.ac.uk> and via email  
274 from [decipher@sanger.ac.uk](mailto:decipher@sanger.ac.uk).

## 275 References

- 276 1. Tilghman JM, Ling AY, Turner TN, Sosa MX, Krumm N, Chatterjee S, et al. Molecular Genetic  
277 Anatomy and Risk Profile of Hirschsprung's Disease. *N Engl J Med*. 2019;380(15):1421-32. PubMed  
278 PMID: 30970187.
- 279 2. Alves MM, Sribudiani Y, Brouwer RW, Amiel J, Antinolo G, Borrego S, et al. Contribution of  
280 rare and common variants determine complex diseases-Hirschsprung disease as a model. *Dev Biol*.  
281 2013;382(1):320-9. Epub 2013/05/28. doi: 10.1016/j.ydbio.2013.05.019. PubMed PMID: 23707863.
- 282 3. Amiel J, Sproat-Emison E, Garcia-Barcelo M, Lantieri F, Burzynski G, Borrego S, et al.  
283 Hirschsprung disease, associated syndromes and genetics: a review. *J Med Genet*. 2008;45(1):1-14.  
284 PubMed PMID: 17965226.
- 285 4. Fewtrell MS, Tam PK, Thomson AH, Fitchett M, Currie J, Huson SM, et al. Hirschsprung's  
286 disease associated with a deletion of chromosome 10 (q11.2q21.2): a further link with the  
287 neurocristopathies? *J Med Genet*. 1994;31(4):325-7. PubMed PMID: 7915329.
- 288 5. Martucciello G, Bicocchi MP, Doderio P, Lerone M, Silengo Cirillo M, Puliti A, et al. Total  
289 colonic aganglionosis associated with interstitial deletion of the long arm of chromosome 10. *Pediatric*  
290 *Surgery International*. 1992;7(4):308-10. doi: 10.1007/bf00183991.
- 291 6. Ederly P, Lyonnet S, Mulligan LM, Pelet A, Dow E, Abel L, et al. Mutations of the RET proto-  
292 oncogene in Hirschsprung's disease. *Nature*. 1994;367(6461):378-80. PubMed PMID: 8114939.
- 293 7. Romeo G, Ronchetto P, Luo Y, Barone V, Seri M, Ceccherini I, et al. Point mutations affecting  
294 the tyrosine kinase domain of the RET proto-oncogene in Hirschsprung's disease. *Nature*.  
295 1994;367(6461):377-8. PubMed PMID: 8114938.
- 296 8. Chatterjee S, Kapoor A, Akiyama JA, Auer DR, Lee D, Gabriel S, et al. Enhancer Variants  
297 Synergistically Drive Dysfunction of a Gene Regulatory Network In Hirschsprung Disease. *Cell*.  
298 2016;167(2):355-68.e10. Epub 2016/10/04. doi: 10.1016/j.cell.2016.09.005. PubMed PMID:  
299 27693352; PubMed Central PMCID: PMC5113733.
- 300 9. Kapoor A, Jiang Q, Chatterjee S, Chakraborty P, Sosa MX, Berrios C, et al. Population  
301 variation in total genetic risk of Hirschsprung disease from common RET, SEMA3 and NRG1  
302 susceptibility polymorphisms. *Human molecular genetics*. 2015;24(10):2997-3003. Epub 2015/02/11.  
303 doi: 10.1093/hmg/ddv051. PubMed PMID: 25666438; PubMed Central PMCID: PMC4406299.
- 304 10. Jiang Q, Arnold S, Heanue T, Kilambi KP, Doan B, Kapoor A, et al. Functional loss of  
305 semaphorin 3C and/or semaphorin 3D and their epistatic interaction with ret are critical to  
306 Hirschsprung disease liability. *Am J Hum Genet*. 2015;96(4):581-96. Epub 2015/04/04. doi:  
307 10.1016/j.ajhg.2015.02.014. PubMed PMID: 25839327; PubMed Central PMCID: PMC4385176.
- 308 11. Garcia-Barcelo MM, Tang CS, Ngan ES, Lui VC, Chen Y, So MT, et al. Genome-wide  
309 association study identifies NRG1 as a susceptibility locus for Hirschsprung's disease. *Proc Natl Acad*  
310 *Sci U S A*. 2009;106(8):2694-9. Epub 2009/02/07. doi: 10.1073/pnas.0809630105. PubMed PMID:  
311 19196962; PubMed Central PMCID: PMC2650328.
- 312 12. Gui H, Tang WK, So MT, Proitsi P, Sham PC, Tam PK, et al. RET and NRG1 interplay in  
313 Hirschsprung disease. *Hum Genet*. 2013;132(5):591-600. Epub 2013/02/13. doi: 10.1007/s00439-013-  
314 1272-9. PubMed PMID: 23400839.
- 315 13. Tang CS, Tang WK, So MT, Miao XP, Leung BM, Yip BH, et al. Fine mapping of the NRG1  
316 Hirschsprung's disease locus. *PLoS One*. 2011;6(1):e16181. Epub 2011/02/02. doi:  
317 10.1371/journal.pone.0016181. PubMed PMID: 21283760; PubMed Central PMCID:  
318 PMC3024406.
- 319 14. Bottani A, Xie YG, Binkert F, Schinzel A. A case of Hirschsprung disease with a chromosome  
320 13 microdeletion, del(13)(q32.3q33.2): potential mapping of one disease locus. *Hum Genet*.  
321 1991;87(6):748-50. PubMed PMID: 1937482.
- 322 15. Kiss P, Osztovcics M. Association of 13q deletion and Hirschsprung's disease. *J Med Genet*.  
323 1989;26(12):793-4. PubMed PMID: 2614805.
- 324 16. Lamont MA, Fitchett M, Dennis NR. Interstitial deletion of distal 13q associated with  
325 Hirschsprung's disease. *J Med Genet*. 1989;26(2):100-4. PubMed PMID: 2918536.
- 326 17. Shanske A, Ferreira JC, Leonard JC, Fuller P, Marion RW. Hirschsprung disease in an infant  
327 with a contiguous gene syndrome of chromosome 13. *Am J Med Genet*. 2001;102(3):231-6. PubMed  
328 PMID: 11484199.
- 329 18. Sparkes RS, Sparkes MC, Kalina RE, Pagon RA, Salk DJ, Distèche CM. Separation of  
330 retinoblastoma and esterase D loci in a patient with sporadic retinoblastoma and del(13)(q14.1q22.3).  
331 *Hum Genet*. 1984;68(3):258-9. PubMed PMID: 6500578.

- 332 19. Puffenberger EG, Hosoda K, Washington SS, Nakao K, deWit D, Yanagisawa M, et al. A  
333 missense mutation of the endothelin-B receptor gene in multigenic Hirschsprung's disease. *Cell*.  
334 1994;79(7):1257-66. Epub 1994/12/30. PubMed PMID: 8001158.
- 335 20. Amiel J, Espinosa-Parrilla Y, Steffann J, Gosset P, Pelet A, Prieur M, et al. Large-scale  
336 deletions and SMADIP1 truncating mutations in syndromic Hirschsprung disease with involvement of  
337 midline structures. *Am J Hum Genet*. 2001;69(6):1370-7. PubMed PMID: 11595972.
- 338 21. Lurie IW, Supovitz KR, Rosenblum-Vos LS, Wulfsberg EA. Phenotypic variability of del(2)  
339 (q22-q23): report of a case with a review of the literature. *Genet Couns*. 1994;5(1):11-4. PubMed  
340 PMID: 8031530.
- 341 22. McMillin KD, Reiss JA, Brown MG, Black MH, Buckmaster DA, Durum CT, et al. Clinical  
342 outcomes of four patients with microdeletion in the long arm of chromosome 2. *Am J Med Genet*.  
343 1998;78(1):36-43. PubMed PMID: 9637421.
- 344 23. Mowat DR, Croaker GD, Cass DT, Kerr BA, Chaitow J, Ades LC, et al. Hirschsprung disease,  
345 microcephaly, mental retardation, and characteristic facial features: delineation of a new syndrome  
346 and identification of a locus at chromosome 2q22-q23. *J Med Genet*. 1998;35(8):617-23. PubMed  
347 PMID: 9719364.
- 348 24. Benailly HK, Lapierre JM, Laudier B, Amiel J, Attie T, De Blois MC, et al. PMX2B, a new  
349 candidate gene for Hirschsprung's disease. *Clin Genet*. 2003;64(3):204-9. PubMed PMID: 12919134.
- 350 25. Wakamatsu N, Yamada Y, Yamada K, Ono T, Nomura N, Taniguchi H, et al. Mutations in  
351 SIP1, encoding Smad interacting protein-1, cause a form of Hirschsprung disease. *Nat Genet*.  
352 2001;27(4):369-70. Epub 2001/03/30. doi: 10.1038/86860. PubMed PMID: 11279515.
- 353 26. Amiel J, Laudier B, Attie-Bitach T, Trang H, de Pontual L, Gener B, et al. Polyalanine  
354 expansion and frameshift mutations of the paired-like homeobox gene PHOX2B in congenital central  
355 hypoventilation syndrome. *Nat Genet*. 2003;33(4):459-61. Epub 2003/03/18. doi: 10.1038/ng1130.  
356 PubMed PMID: 12640453.
- 357 27. Amiel J, Lyonnet S. Hirschsprung disease, associated syndromes, and genetics: a review. *J*  
358 *Med Genet*. 2001;38(11):729-39. PubMed PMID: 11694544.
- 359 28. Brewer C, Holloway S, Zawalnyski P, Schinzel A, FitzPatrick D. A chromosomal deletion map  
360 of human malformations. *Am J Hum Genet*. 1998;63(4):1153-9. PubMed PMID: 9758599.
- 361 29. Brewer C, Holloway S, Zawalnyski P, Schinzel A, FitzPatrick D. A chromosomal duplication  
362 map of malformations: regions of suspected haplo- and triplolethality--and tolerance of segmental  
363 aneuploidy--in humans. *Am J Hum Genet*. 1999;64(6):1702-8. PubMed PMID: 10330358.
- 364 30. Mahboubi S, Templeton JM, Jr. Association of Hirschsprung's disease and imperforate anus in  
365 a patient with "cat-eye" syndrome. A report of one case and review of the literature. *Pediatr Radiol*.  
366 1984;14(6):441-2. PubMed PMID: 6504608.
- 367 31. Kerstjens-Frederikse WS, Hofstra RM, van Essen AJ, Meijers JH, Buys CH. A Hirschsprung  
368 disease locus at 22q11? *J Med Genet*. 1999;36(3):221-4. PubMed PMID: 10204849.
- 369 32. Coe BP, Witherspoon K, Rosenfeld JA, van Bon BW, Vulto-van Silfhout AT, Bosco P, et al.  
370 Refining analyses of copy number variation identifies specific genes associated with developmental  
371 delay. *Nat Genet*. 2014;46(10):1063-71. PubMed PMID: 25217958.
- 372 33. Cooper GM, Coe BP, Girirajan S, Rosenfeld JA, Vu TH, Baker C, et al. A copy number  
373 variation morbidity map of developmental delay. *Nat Genet*. 2011;43(9):838-46. PubMed PMID:  
374 21841781.
- 375 34. Lek M, Karczewski KJ, Minikel EV, Samocha KE, Banks E, Fennell T, et al. Analysis of  
376 protein-coding genetic variation in 60,706 humans. *Nature*. 2016;536(7616):285-91. PubMed PMID:  
377 27535533.
- 378 35. Ruderfer DM, Hamamsy T, Lek M, Karczewski KJ, Kavanagh D, Samocha KE, et al. Patterns  
379 of genic intolerance of rare copy number variation in 59,898 human exomes. *Nat Genet*.  
380 2016;48(10):1107-11. Epub 2016/08/18. doi: 10.1038/ng.3638. PubMed PMID: 27533299; PubMed  
381 Central PMCID: PMC5042837.
- 382 36. Gui H, Schriemer D, Cheng WW, Chauhan RK, Antinolo G, Berrios C, et al. Whole exome  
383 sequencing coupled with unbiased functional analysis reveals new Hirschsprung disease genes.  
384 *Genome Biol*. 2017;18(1):48. Epub 2017/03/10. doi: 10.1186/s13059-017-1174-6  
385 10.1186/s13059-017-1174-6 [pii]. PubMed PMID: 28274275; PubMed Central PMCID: PMC5343413.
- 386 37. Tang CS, Li P, Lai FP, Fu AX, Lau ST, So MT, et al. Identification of Genes Associated With  
387 Hirschsprung Disease, Based on Whole-Genome Sequence Analysis, and Potential Effects on Enteric  
388 Nervous System Development. *Gastroenterology*. 2018;155(6):1908-22.e5. Epub 2018/09/16. doi:  
389 10.1053/j.gastro.2018.09.012. PubMed PMID: 30217742.

- 390 38. Rosenfeld JA, Coe BP, Eichler EE, Cuckle H, Shaffer LG. Estimates of penetrance for  
391 recurrent pathogenic copy-number variations. *Genet Med*. 2013;15(6):478-81. Epub 2012/12/22. doi:  
392 10.1038/gim.2012.164. PubMed PMID: 23258348; PubMed Central PMCID: PMC3664238.
- 393 39. Ballif BC, Theisen A, Rosenfeld JA, Traylor RN, Gastier-Foster J, Thrush DL, et al.  
394 Identification of a recurrent microdeletion at 17q23.1q23.2 flanked by segmental duplications  
395 associated with heart defects and limb abnormalities. *Am J Hum Genet*. 2010;86(3):454-61. PubMed  
396 PMID: 20206336.
- 397 40. Laurell T, Lundin J, Anderlid BM, Gorski JL, Grigelioniene G, Knight SJ, et al. Molecular and  
398 clinical delineation of the 17q22 microdeletion phenotype. *Eur J Hum Genet*. 2013;21(10):1085-92.  
399 PubMed PMID: 23361222.
- 400 41. Tang CS, Gui H, Kapoor A, Kim JH, Luzon-Toro B, Pelet A, et al. Trans-ethnic meta-analysis  
401 of genome-wide association studies for Hirschsprung disease. *Human molecular genetics*.  
402 2016;25(23):5265-75. Epub 2016/10/06. doi: 10.1093/hmg/ddw333. PubMed PMID: 27702942.
- 403 42. de Pontual L, Pelet A, Trochet D, Jaubert F, Espinosa-Parrilla Y, Munnich A, et al. Mutations  
404 of the RET gene in isolated and syndromic Hirschsprung's disease in human disclose major and  
405 modifier alleles at a single locus. *J Med Genet*. 2006;43(5):419-23. Epub 2006/01/31. doi:  
406 10.1136/jmg.2005.040113. PubMed PMID: 16443855; PubMed Central PMCID: PMC2649010.
- 407 43. de Pontual L, Pelet A, Clement-Ziza M, Trochet D, Antonarakis SE, Attie-Bitach T, et al.  
408 Epistatic interactions with a common hypomorphic RET allele in syndromic Hirschsprung disease.  
409 *Hum Mutat*. 2007;28(8):790-6. Epub 2007/04/03. doi: 10.1002/humu.20517. PubMed PMID:  
410 17397038.
- 411 44. de Pontual L, Zaghloul NA, Thomas S, Davis EE, McGaughey DM, Dollfus H, et al. Epistasis  
412 between RET and BBS mutations modulates enteric innervation and causes syndromic Hirschsprung  
413 disease. *Proc Natl Acad Sci U S A*. 2009;106(33):13921-6. Epub 2009/08/12. doi:  
414 10.1073/pnas.0901219106. PubMed PMID: 19666486; PubMed Central PMCID: PMC2728996.
- 415 45. Arnold S, Pelet A, Amiel J, Borrego S, Hofstra R, Tam P, et al. Interaction between a  
416 chromosome 10 RET enhancer and chromosome 21 in the Down syndrome-Hirschsprung disease  
417 association. *Hum Mutat*. 2009;30(5):771-5. Epub 2009/03/24. doi: 10.1002/humu.20944. PubMed  
418 PMID: 19306335; PubMed Central PMCID: PMC2779545.
- 419 46. Jannot AS, Pelet A, Henrion-Caude A, Chaoui A, Masse-Morel M, Arnold S, et al.  
420 Chromosome 21 scan in Down syndrome reveals DSCAM as a predisposing locus in Hirschsprung  
421 disease. *PLoS One*. 2013;8(5):e62519. Epub 2013/05/15. doi: 10.1371/journal.pone.0062519.  
422 PubMed PMID: 23671607; PubMed Central PMCID: PMC3646051.
- 423 47. Natarajan D, Marcos-Gutierrez C, Pachnis V, de Graaff E. Requirement of signalling by  
424 receptor tyrosine kinase RET for the directed migration of enteric nervous system progenitor cells  
425 during mammalian embryogenesis. *Development*. 2002;129(22):5151-60. Epub 2002/10/26. PubMed  
426 PMID: 12399307.
- 427 48. Yamagishi H, Garg V, Matsuoka R, Thomas T, Srivastava D. A molecular pathway revealing a  
428 genetic basis for human cardiac and craniofacial defects. *Science*. 1999;283(5405):1158-61. PubMed  
429 PMID: 10024240.
- 430 49. Hendershot TJ, Liu H, Sarkar AA, Giovannucci DR, Clouthier DE, Abe M, et al. Expression of  
431 Hand2 is sufficient for neurogenesis and cell type-specific gene expression in the enteric nervous  
432 system. *Dev Dyn*. 2007;236(1):93-105. PubMed PMID: 17075884.
- 433 50. D'Autreaux F, Margolis KG, Roberts J, Stevanovic K, Mawe G, Li Z, et al. Expression level of  
434 Hand2 affects specification of enteric neurons and gastrointestinal function in mice. *Gastroenterology*.  
435 2011;141(2):576-87, 87 e1-6. PubMed PMID: 21669203.
- 436 51. Pan L, Ma X, Wen B, Su Z, Zheng X, Liu Y, et al. Microphthalmia-associated transcription  
437 factor/T-box factor-2 axis acts through Cyclin D1 to regulate melanocyte proliferation. *Cell Prolif*.  
438 2015;48(6):631-42. Epub 2015/10/22. doi: 10.1111/cpr.12227. PubMed PMID: 26486273.
- 439 52. Stanchina L, Baral V, Robert F, Pingault V, Lemort N, Pachnis V, et al. Interactions between  
440 Sox10, Edn3 and Ednrb during enteric nervous system and melanocyte development. *Dev Biol*.  
441 2006;295(1):232-49. Epub 2006/05/03. doi: 10.1016/j.ydbio.2006.03.031. PubMed PMID: 16650841.
- 442 53. Watanabe Y, Stanchina L, Lecerf L, Gacem N, Conidi A, Baral V, et al. Differentiation of  
443 Mouse Enteric Nervous System Progenitor Cells Is Controlled by Endothelin 3 and Requires  
444 Regulation of Ednrb by SOX10 and ZEB2. *Gastroenterology*. 2017;152(5):1139-50.e4. Epub  
445 2017/01/09. doi: 10.1053/j.gastro.2016.12.034. PubMed PMID: 28063956.
- 446 54. Miao X, Leon TY, Ngan ES, So MT, Yuan ZW, Lui VC, et al. Reduced RET expression in gut  
447 tissue of individuals carrying risk alleles of Hirschsprung's disease. *Human molecular genetics*.  
448 2010;19(8):1461-7. Epub 2010/01/22. doi: 10.1093/hmg/ddq020. PubMed PMID: 20089534.

- 449 55. Jiang Q, Ho YY, Hao L, Nichols Berrios C, Chakravarti A. Copy number variants in candidate  
450 genes are genetic modifiers of Hirschsprung disease. *PLoS One*. 2011;6(6):e21219. Epub  
451 2011/06/30. doi: 10.1371/journal.pone.0021219. PubMed PMID: 21712996; PubMed Central PMCID:  
452 PMCPMC3119685.
- 453 56. Tang CS, Cheng G, So MT, Yip BH, Miao XP, Wong EH, et al. Genome-wide copy number  
454 analysis uncovers a new HSCR gene: NRG3. *PLoS Genet*. 2012;8(5):e1002687. Epub 2012/05/17.  
455 doi: 10.1371/journal.pgen.1002687. PubMed PMID: 22589734; PubMed Central PMCID:  
456 PMCPMC3349728.
- 457 57. Brosens E, Marsch F, de Jong EM, Zaveri HP, Hilger AC, Choinitzki VG, et al. Copy number  
458 variations in 375 patients with oesophageal atresia and/or tracheoesophageal fistula. *Eur J Hum*  
459 *Genet*. 2016;24(12):1715-23. PubMed PMID: 27436264.
- 460 58. Lai FP, Lau ST, Wong JK, Gui H, Wang RX, Zhou T, et al. Correction of Hirschsprung-  
461 Associated Mutations in Human Induced Pluripotent Stem Cells Via Clustered Regularly Interspaced  
462 Short Palindromic Repeats/Cas9, Restores Neural Crest Cell Function. *Gastroenterology*.  
463 2017;153(1):139-53 e8. doi: 10.1053/j.gastro.2017.03.014. PubMed PMID: 28342760.
- 464 59. Brouwer RWW, van den Hout M, Kockx CEM, Brosens E, Eussen B, de Klein A, et al.  
465 Nimbus: A design-driven analyses suite for amplicon based NGS data. *Bioinformatics*. 2018. Epub  
466 2018/03/15. doi: 10.1093/bioinformatics/bty145. PubMed PMID: 29538618.
- 467 60. Brouwer RW, van den Hout MC, Grosveld FG, van Ijcken WF. NARWHAL, a primary analysis  
468 pipeline for NGS data. *Bioinformatics*. 2012;28(2):284-5. Epub 2011/11/11. doi:  
469 10.1093/bioinformatics/btr613. PubMed PMID: 22072383.
- 470 61. Halim D, Brosens E, Muller F, Wangler MF, Beaudet AL, Lupski JR, et al. Loss-of-Function  
471 Variants in MYLK Cause Recessive Megacystis Microcolon Intestinal Hypoperistalsis Syndrome. *Am J*  
472 *Hum Genet*. 2017;101(1):123-9. Epub 2017/06/13. doi: 10.1016/j.ajhg.2017.05.011. PubMed PMID:  
473 28602422; PubMed Central PMCID: PMCPMC5501771.
- 474 62. Schriemer D, Sribudiani Y, A IJ, Natarajan D, MacKenzie KC, Metzger M, et al. Regulators of  
475 gene expression in Enteric Neural Crest Cells are putative Hirschsprung disease genes. *Dev Biol*.  
476 2016;416(1):255-65. PubMed PMID: 27266404.
- 477 63. Memic F, Knoflach V, Morarach K, Sadler R, Laranjeira C, Hjerling-Leffler J, et al.  
478 Transcription and Signaling Regulators in Developing Neuronal Subtypes of Mouse and Human  
479 Enteric Nervous System. *Gastroenterology*. 2018;154(3):624-36. PubMed PMID: 29031500.
- 480 64. McCann CJ, Alves MM, Brosens E, Natarajan D, Perin S, Chapman C, et al. Neuronal  
481 Development and Onset of Electrical Activity in the Human Enteric Nervous System.  
482 *Gastroenterology*. 2019. Epub 2019/01/06. doi: 10.1053/j.gastro.2018.12.020. PubMed PMID:  
483 30610864.
- 484 65. Zhan X, Hu Y, Li B, Abecasis GR, Liu DJ. RVTESTS: an efficient and comprehensive tool for  
485 rare variant association analysis using sequence data. *Bioinformatics*. 2016;32(9):1423-6. PubMed  
486 PMID: 27153000.
- 487 66. Nechiporuk A, Linbo T, Poss KD, Raible DW. Specification of epibranchial placodes in  
488 zebrafish. *Development*. 2007;134(3):611-23. PubMed PMID: 17215310.
- 489 67. Kuil LE, Oosterhof N, Geurts SN, van der Linde HC, Meijering E, van Ham TJ. Reverse  
490 genetic screen reveals that I134 facilitates yolk sac macrophage distribution and seeding of the brain.  
491 *Dis Model Mech*. 2019;12(3). PubMed PMID: 30765415.
- 492 68. Hoshijima K, Jurynek MJ, Klatt Shaw D, Jacobi AM, Behlke MA, Grunwald DJ. Highly Efficient  
493 CRISPR-Cas9-Based Methods for Generating Deletion Mutations and F0 Embryos that Lack Gene  
494 Function in Zebrafish. *Dev Cell*. 2019;51(5):645-57 e4. PubMed PMID: 31708433.
- 495 69. Heanue TA, Pachnis V. Ret isoform function and marker gene expression in the enteric  
496 nervous system is conserved across diverse vertebrate species. *Mech Dev*. 2008;125(8):687-99.  
497 PubMed PMID: 18565740.
- 498 70. Firth HV, Richards SM, Bevan AP, Clayton S, Corpas M, Rajan D, et al. DECIPHER:  
499 Database of Chromosomal Imbalance and Phenotype in Humans Using Ensembl Resources. *Am J*  
500 *Hum Genet*. 2009;84(4):524-33. PubMed PMID: 19344873.

501

502 **Figure legends**

503 **Figure 1. Schematic overview of our overall study design and methods used.** a) *In brief: We*  
504 *determined the Copy Number profiles of different subgroups of HSCR patients (1-3) and controls (4).*  
505 *We determined RET and / or known disease gene coding mutations and ranked the genes affected by*  
506 *a CNV according to frequency in controls, expression in the developing mouse ENS and gene tolerance*  
507 *to variation. Next, we determined whether disruption of the main candidate genes resulted in a reduction*  
508 *of enteric neurons in zebrafish. b) In parallel, we evaluated the contribution of different genetic risk*  
509 *factors, by comparing the contribution of known non-coding predisposing haplotypes across groups. o/e*  
510 *= overexpressed, VI = intolerant to variation.*

511 **Figure 2. ENS overexpressed genes intolerant to variation were enriched in HSCR-complex**  
512 **patients and their disruption in zebrafish caused HSCR phenotypes** a) *Graph showing CNV size,*  
513 *each dot represents a CNV. b) graph showing the number of variant intolerant (VI) genes overexpressed*  
514 *in the mouse ENS per patient, each dot represents one patient. c) Graph showing the RSnc, each dot*  
515 *represents one patient. Error bars represent standard deviation, statistical analysis used: students t-test*  
516 *(a-c). d) CRISPR/Cas9 complex injections in zebrafish fertilized eggs induced HSCR phenotypes upon*  
517 *disruption of four genes (accumulated data from multiple experiments). e) Graph showing accumulated*  
518 *data of the percentage of fish with HSCR phenotypes upon injection of a morpholino targeting Ret*  
519 *translation at a concentration that induced HSCR phenotypes in approximately 50% of the fish. Ret*  
520 *morpholino injections in combination with disruption of mapk8 shows epistasis. Disruption of gnl1*  
521 *showed a trend towards higher penetrance of HSCR phenotypes. f) A second injection round targeting*  
522 *gnl1, using a lower dose of ret morpholino, confirmed gnl1 epistasis with Ret.*

523 **Figure 3. Complex HSCR genetics: genetic predispositions of HSCR patient groups** a) *Visual*  
524 *representation of the distribution of genetic predispositions over HSCR patient groups. In total 197*  
525 *patients born between 1973 and 2018 were evaluated by a clinical geneticist in the department of*  
526 *Clinical Genetics, Erasmus Medical Center, Rotterdam. Of these, 114 did not have associated*  
527 *anomalies nor a known syndrome. 29 patients had a known HSCR related genetic syndrome, including*  
528 *Down syndrome (n=18). 153 out of 197 patients were genetically evaluated for RET gene involvement*  
529 *and 21 had a pathogenic RET variant. b) Pie charts showing the incidence of rare CNVs containing*  
530 *genes overexpressed in the developing mouse ENS and coding variants in HSCR patients. c) Graphical*



531 *representation of a hypothetical model explaining the relative contributions of the risk scores in our 3*  
532 *patient groups. Error bars represent standard deviation.*

533 **Table 1. Genes in rare CN losses that are overexpressed in mouse ENS and intolerant to**  
534 **genetic variation** *Genes marked with an # also have a loss of function variant in an independent*  
535 *HSCR cohort (see table 2). Depicted are the RSnc (see S11) and the CNV and variant intolerance*  
536 *scores derived from <http://gnomad.broadinstitute.org/> and <http://exac.broadinstitute.org/about>.*

537

538 **Table 2: WES: Nonsense and splice site variants in rare CNV genes**

539 *Rare putative deleterious nonsense variants and variants predicted to affect splicing in a whole exome*  
540 *sequencing cohort of HSCR (n=76, 149 controls) [36] and whole genome sequencing cohort of 443*  
541 *short segment HSCR patients and 493 unaffected controls[37]. Variants in genes intolerant to*  
542 *variation that were also impacted by the de novo 17q23.1 - q23.2 loss (INTS2, MED13), the de novo*  
543 *6p22.1 - p21.33 loss (PRRC2A, TUBB) , the 9p21 loss (LINGO2), the maternal inherited 10q11.22 -*  
544 *q11.23 loss (SGMS1), de novo 7q36.1 gain (KMT2C) and the 3q24 gain (SLC6A6).*

**Table 1. Genes in rare CN losses that are overexpressed in mouse ENS and intolerant to genetic variation**

Patient	RS <sub>NC</sub>	Gene	<i>ExAC/ GnomAD intolerance scores</i>				CNV region
			Missense Z	pLI	Deletion single	Deletion CNV	
P_000479	4,16	<i>SLC8A1</i>	2.23	1.00	-0.02	0.31	chr2:40,624,267-40,646,501
P_000512	8,31	<i>TUBB#</i>	5.71	0.98	-2.85	-1.72	chr6:28,005,012-31,683,185
		<i>GNL1</i>	2.52	1.00	1.03	0.70	
		<i>GABBR1</i>	4.98	1.00	1.36	1.23	
P_000537	6,92	<i>MAPK8</i>	2.92	1.00	0.84	-2.25	chr10: 49,033,586 -52,431,193
P_000561	6,08	<i>UFD1L</i>	2.77	1.00	1.06	-2.53	chr22:18,861,209-21,630,630
P_000567	7,98	<i>TBX2</i>	1.75	0.99	-0.01	0.53	chr17:58,076,721-60,362,868
		<i>USP32</i>	3.55	1.00	-2.85	-0.93	
P_002431	9,37	<i>AKT3</i>	4.03	1.00	-2.61	-1.20	chr1:243,963,527-244,016,804

**Table 2: WES: Nonsense and splice site variants in rare CNV genes in HSCR patients**

Sample	Chr	Start	Stop	Ref	Alt	Exon	Gene	Type	location	Effect	HGVS cDNA-level	CADD	gnomADv2.1	gnomADV2.1
													Exomes	Genomes
SE14-0527	17	59946466	59946466	.	T	23	<i>INTS2</i>	insertion	exonic	frameshift	NM_001330417.1:c.3172dupA	.	0	0
HK19-0006	17	60072727	60072727	C	T	10	<i>MED13</i>	snv	intronic	splicing	NM_005121:c.1968-1G>A	22.4	0	0
SE16-3114	17	59469360	59469360	C	T	26	<i>BCAS3</i>	snv	exonic	stopgain	NM_001320470.1:c.2773C>T	18.4	0.0002	0.0007
SE14-0656	6	31604286	31604286	G	T	27	<i>PRRC2A</i>	snv	splicing	splicing	NM_004638.3:c.5836-1G>T	23.6	0.0001	3.24E-05
SE16-3123	6	30692109	30692110	CA	A	4	<i>TUBB</i>	substitution	exonic	frameshift	NM_001293212.1:c.1330_1331delCAinsA	.	0	0
SE17-3220	7	151962296	151962296	T	C	8	<i>KMT2C</i>	snv	splicing	splicing	NM_170606.2:c.1013-2A>G	22	8.21E-06	0
HK19-0002	9	28476025	28476025	T	G		<i>LINGO2</i>	snv	intronic	splicing	NM_001258282:c.-395-2A>C	23.2	0	0
HK19-0003	10	52103343	52103344	TA	T	7	<i>SGMS1</i>	deletion	exonic	frameshift	NM_147156:c.T529delT;p.F177del	33	0	0
HK19-0004	10	52104106	52104108	CTG	C		<i>SGMS1</i>	deletion	intronic	splicing	NM_147156:c.-313-2CAG>--G	24.5	0	0
HK19-0005	10	52349911	52349911	A	G		<i>SGMS1</i>	snv	intronic	splicing	NM_147156:c.-683+2T>C	23	0	0
SE16-3109	22	21065731	21065731	G	A	51	<i>PI4KA</i>	snv	exonic	stopgain	NM_058004.3:c.5821C>T	51	0.0002	0.0002
HK19-0001	3	14485130	14485130	A	G		<i>SLC6A6</i>	snv	intronic	splicing	NM_001134367:c.297-6A>G	15.92	0	0

**Figure 1**

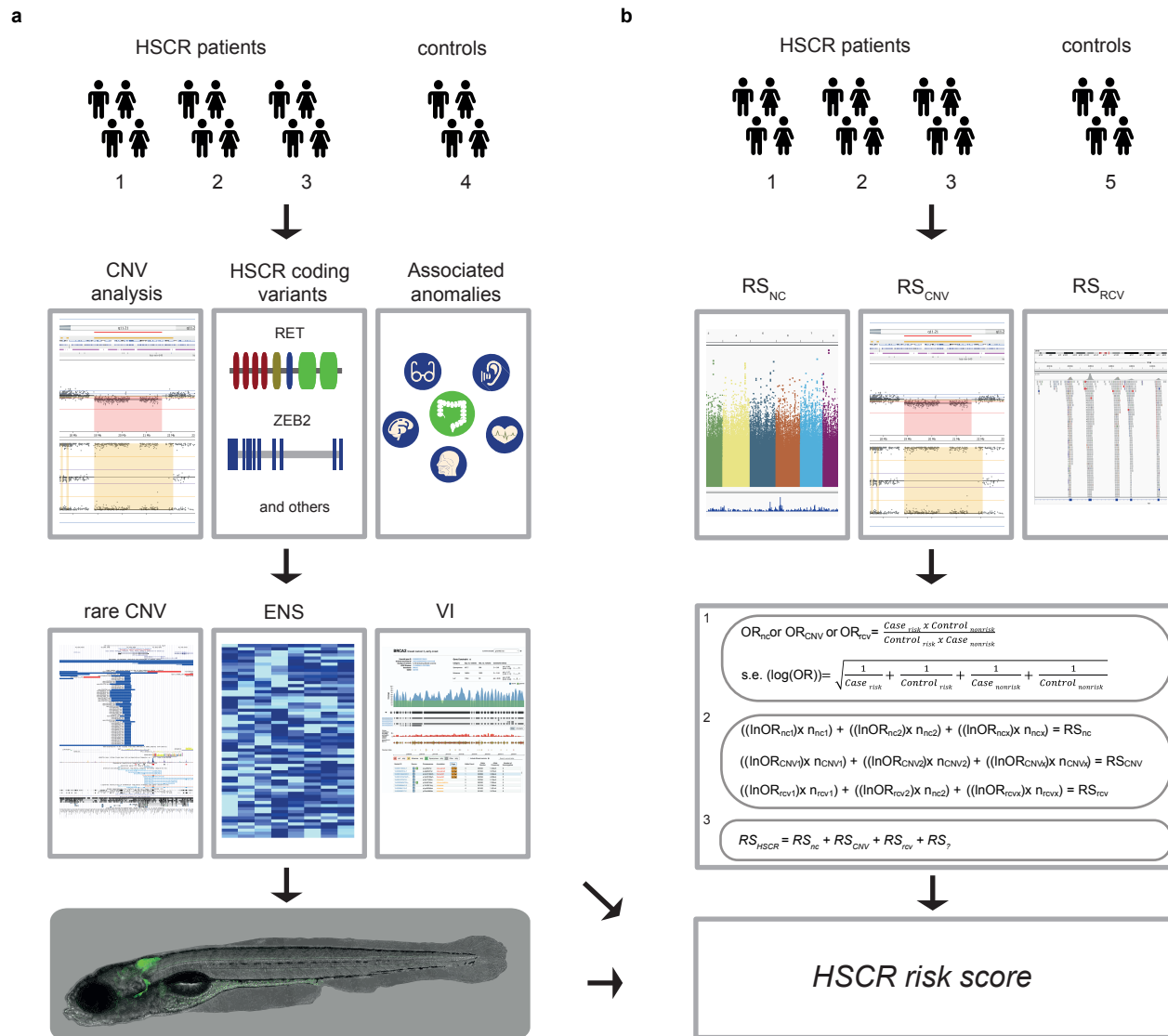


## Figure 2

It is made available under a [CC-BY-NC-ND 4.0 International license](https://creativecommons.org/licenses/by-nc-nd/4.0/).

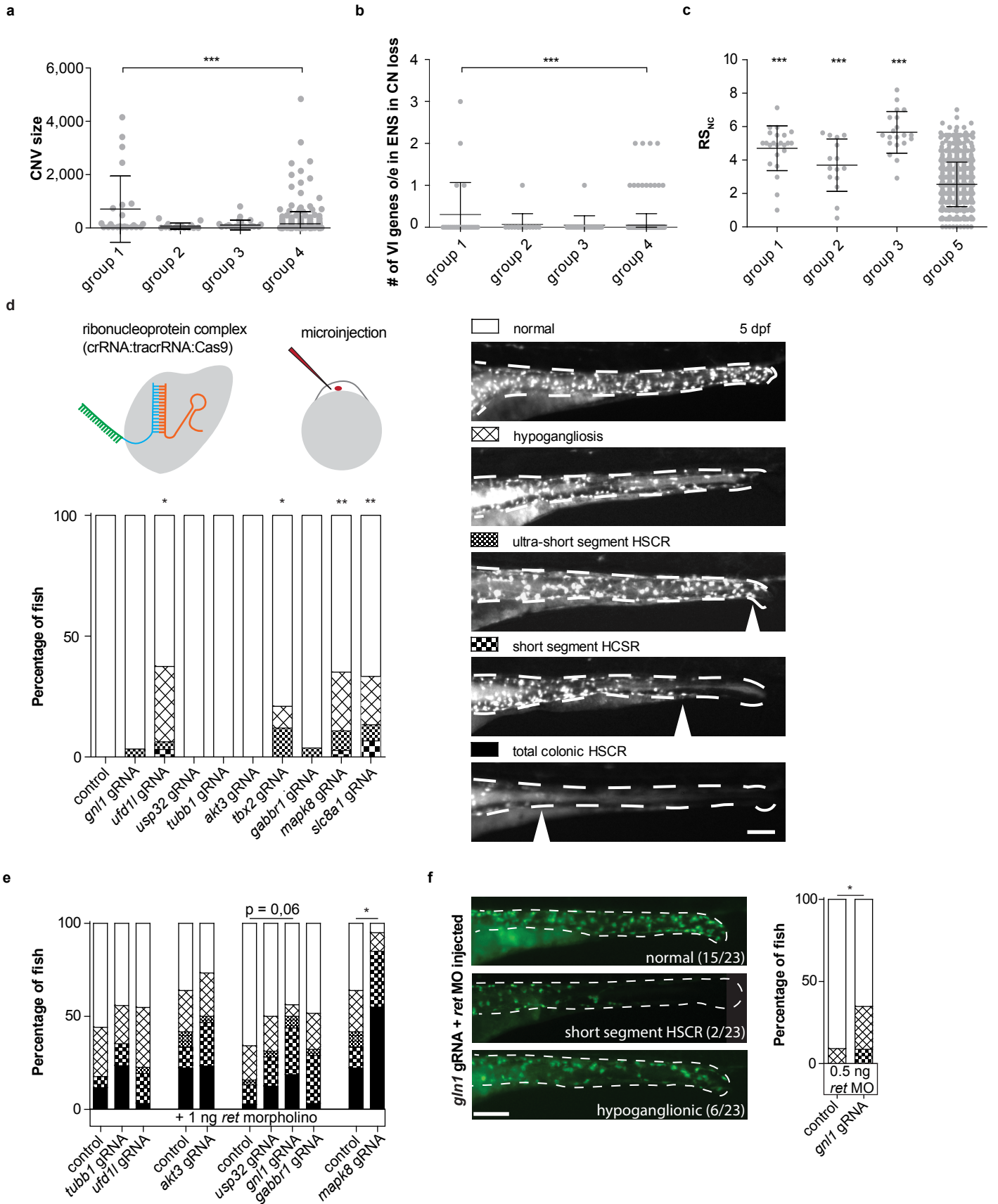


**Figure 3**

